Using the Bond Valence Sum Model to calculate Li-diffusion pathways in Silicene with MgX2 (X=Cl, Br, I) substrates

Papadopoulou, K, Chroneos, A & Christopoulos, S

Using the Bond Valence Sum Model to calculate Li-diffusion pathways in Silicene with MgX₂ (X=Cl, Br, I) substrates

Konstantina A. Papadopoulou,[1, 2] Alexander Chroneos,[3, 4] and Stavros-Richard G. Christopoulos[5, 6, ∗]

[1]*Department of Physics and Astronomy, Faculty of Environment,
Science and Economy, University of Exeter, EX4 4QL, Exeter, UK*
[2]*Faculty of Engineering, Environment and Computing,
Coventry University, Priory Street, Coventry, CV1 5FB, United Kingdom*
[3]*Department of Electrical and Computer Engineering, University of Thessaly, 38221 Volos, Greece*
[4]*Department of Materials, Imperial College London, London SW7 2BP, UK*
[5]*Department of Computer Science, School of Computing and Engineering,
University of Huddersfield, HD4 6DJ, Huddersfield, UK*
[6]*Centre for Computational Science and Mathematical Modelling, Coventry University, Coventry CV1 2TU, UK*

Using the BVS method we calculate Li-ion pathways and diffusion barriers in the interface between silicene and $MgCl_2$, $MgBr_2$ and MgI_2 substrates and we show that the results are in good agreement with previously published DFT studies. In addition, we showcase that BVS does not need the exact crystal structure as we examine different initial positions for the Li ion and different interface heights without affecting the calculated $BVSE$. Furthermore, we show that surface diffusion BVS calculations can be used to roughly optimize the interface, thus completely foregoing DFT geometry optimization calculations. Here, we propose that BVS can substitute DFT as a quick filter when searching for low migration barriers in silicene-based materials, providing good enough accuracy.
Keywords: Bond Valence Sum, Conductive Pathways, Li diffusion, Energy Barrier, Silicene

I. INTRODUCTION

Two-dimensional (2D) materials have attracted considerable attention in recent years for improving the performance of electronic devices[1–7]. This is mainly due to newly-found properties regarding their electronic conductivity, interaction with light, and even mechanical properties and chemical reactivity. Among these materials is silicene, the 2D result of silicon, which has emerged as the most preferable 2D material because of its compatibility with silicon-based technology[8].

Unlike graphene which has a planar structure, silicene exhibits a two-layered structure with two Si sub-lattices forming hexagonal rings. This geometry allows silicene a stronger spin – orbit coupling (SOC) effect which results to a more prominent Quantum Spin Hall effect (QSHE) under different hydrostatic strains due to an increasing gap size[9]. In addition, due to its structure, silicene is predicted to be a gapless semiconductor. The two formed Si layers allow to tune its electronic properties and even open an energy gap by applying an electrical field perpendicular to the silicene sheet, thus creating charge transfer between the Si layers[10,11]. Germanene, the other 2D "cousin" of graphene that also has a two-layered structure, has SOC effect almost ten times larger than silicene[12], thus larger gap size (1.9 meV in silicene versus 33 meV in germanene[13]).

Despite the many interesting properties of silicene, most studies remain theoretical since the synthesis of silicene in bulk has not yet been achieved[8]. This is mainly due to the fact that there is no graphite-like Si allotrope[10]. The most frequently used computational method to model silicene is Density Functional Theory (DFT)[14], which can describe the electron-ion interactions[15] using pseudopotentials[16] generated on the fly. In addition, DFT has also been used to examine the effects of a substrate on the electronic properties of silicene[17–22].

Despite DFT's many advantages, especially regarding accuracy[23], it is computationally intensive. Instead, the Bond Valence Sum (BVS) model has started being used to predict or validate new crystal structures[24,25] and to calculate diffusion pathways and migration energy barriers for mobile ions in crystals[26–28].

BVS takes advantage of Pauling's electrostatic valence principle[29] where the sum of bond valences, s_{ij}, around a given ion i, is equal to its total ionic valence, V_i, i.e., its charge. Additionally, in BVS the exact coordinates of the ions are not required[30].

For the calculation of possible sites a moving ion can exist in the material's structure, BVS uses the following empirical relationship for a cation A connected to an anion X with the bond length between them denoted as R[23,31]:

$$S_{A-X} = exp[(R_0 - R)/b] \qquad (1)$$

where S is the experimental bond valence, whereas R_0 (for ion sizes) and b (for softness) are fitted parameters. For most of the ionic bonds, $b = 0.37$[30]. At each arbitrary site the ion occupies, if the BVS is equal to the moving ion's oxidation number, then that is a site belonging to the migration pathway of the ion. The model also allows for small displacements using the valence mismatch[31], $|\Delta V|$, which is in the range of $[0.05, 0.2]$ valence units[30].

The calculated sites are drawn as contour maps signifying the pathways inside the crystal structures. We have, therefore, isosurfaces with fixed $|\Delta V|$ denoting regions inside the crystal structures where a certain activation

energy E_{act} may be reached. The Bond Valence Site Energy, $BVSE$, for the mobile cation A is given by[25,32]:

$$BVSE = D_0 \left[\sum_{j=1}^{N_X} \frac{(s_{A-X_j} - s_{min})^2}{s_{min}^2} - N \right] + E_{repulsion}$$

(2)

where D_0 is the bond dissociation energy, N is the anions (X) number the cation bonds with, $E_{repulsion}$ is a penalty term due to repulsions[33] (Coulombic) and s_{min} is the valence corresponding to the distance between A and X[33] in equilibrium.

It is the scope of this paper to examine whether the BVS model can substitute DFT when it comes to calculating Li-ion migration energy barriers and pathways in silicene. BVS should allow for less computational time and good accuracy[23] when compared to DFT, so that the latter can target only potentially interesting materials and not lose time analysing a high number of structures.

We use MgX_2 (X=Cl, Br, I) as substrates as proposed by Zhu et al.[34], and examine Li diffusion in the interface between the substrates and silicene. We compare our results with those from DFT calculations[34] and also discuss the differences between surface and interface BVS calculations.

II. COMPUTATIONAL METHODS

We chose to forgo DFT calculations in order to take advantage of the fact that the BVS model does not need to know the exact crystal structure, therefore no structure optimisation is needed. Instead, we introduced a vacuum space of 15Å between adjacent MgX_2 (X=Cl, Br, I) layers to minimize the mirror interactions of the upper and bottom layers, and placed a silicene layer on top of the substrates at different distances. Finally, a Li ion was placed in the interface at a distance from the MgX_2 surface which, although arbitrary, was smaller than the bond length between Li-Cl, Li-Br and Li-I for each case.

To start with, for the $MgCl_2$ and $MgBr_2$ substrates the Li ion was placed at the hollow site, i.e., below the center of a Si hexagon, while for the MgI_2 the Li ion was placed at the top site, i.e., below a Si atom belonging in the upper of the two silicene levels. These are the positions suggested by Zhu et al.[34].

For the calculation of the bond valence sums, we used the command line form of the softBV software[23] and the parameters available therein[35]. Valid sites for the Li-ion to occupy were considered those where the total valence sum was within ± 0.2 valence units of Li's natural oxidation number (+1).

III. RESULTS

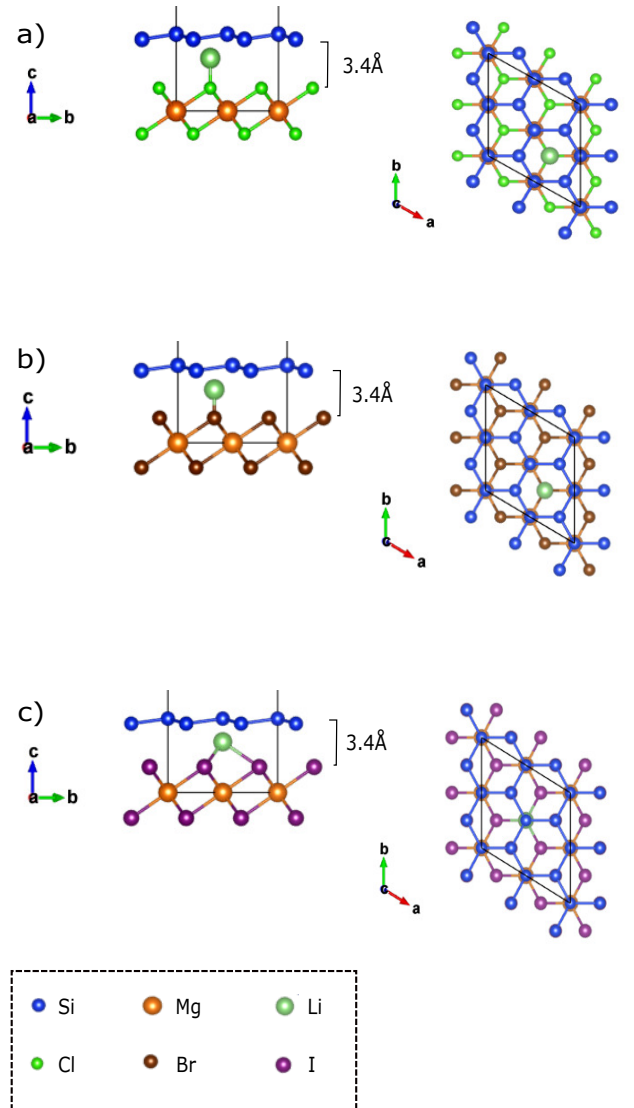In Figure 1 we can see the considered structures for the silicene with the substrates and the Li ion in the

FIG. 1: The $2 \times 2 \times 1$ supercell for the silicene with a)$MgCl_2$ substrate, b)$MgBr_2$ substrate and c)MgI_2 substrate, and a Li ion (green sphere) in the interface. Left panels: Front view. Right panels: Top view. Light brown spheres: Mg. Light green spheres: Cl. Brown spheres: Br. Purple spheres: I. Blue spheres: Si.

interface. The hollow and top sites described in Section II can also be seen. The interface is 3.4Å .

For the case with a $MgCl_2$ substrate, the application of the BVS method showed that the energetically most favourable pathway for the Li-ion to migrate in the interface is the hollow - top - hollow one, i.e., starting and ending at a hollow site, with the transition state being at a top site. The $BVSE$ was 0.15 eV. The pathways and the $BVSE$ are shown in Fig. 2 where we can see that the BVS has calculated three equivalent pathways energy-wise.

For the case with a $MgBr_2$ substrate, the application of the BVS method showed that the energetically most favourable pathway for the Li-ion to migrate in the in-
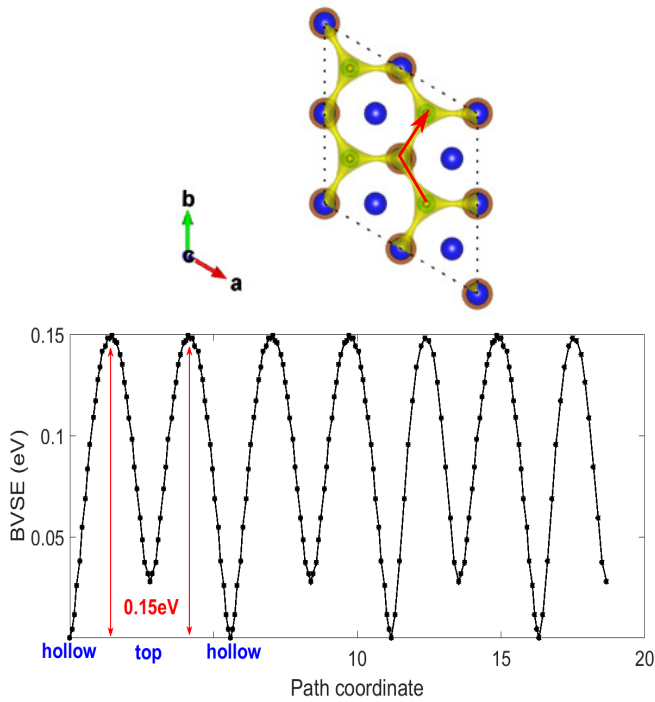
FIG. 2: Top panel: Top view of the $2 \times 2 \times 1$ supercell for the silicene with a $MgCl_2$ substrate and the Li conductive pathways (yellow surface) as calculated by the BVS method. The arrow shows the direction of the migration. Bottom panel: The $BVSE$. Light brown spheres: Mg. Light green spheres: Cl. Blue spheres: Si.
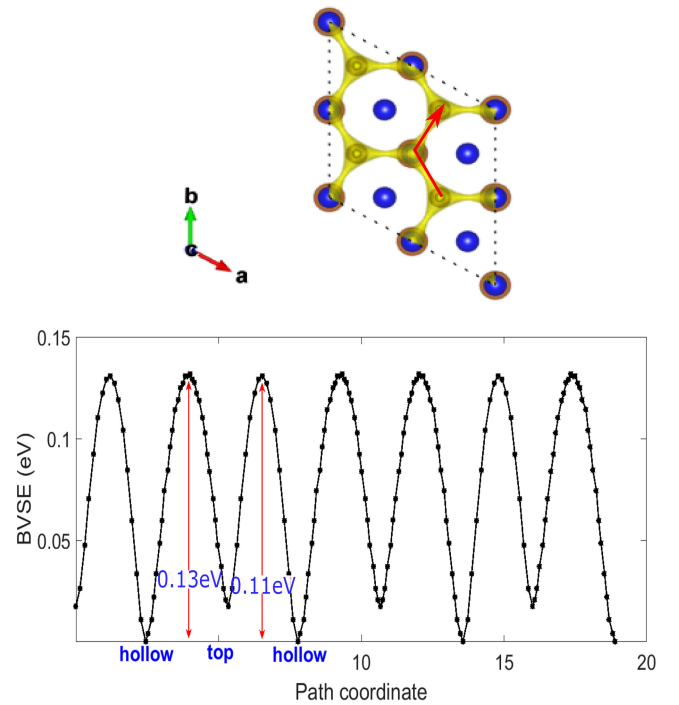

FIG. 3: Top panel: Top view of the $2 \times 2 \times 1$ supercell for the silicene with a $MgBr_2$ substrate and the Li conductive pathways (yellow surface) as calculated by the BVS method. The arrow shows the direction of the migration. Bottom panel: The $BVSE$. Light brown spheres: Mg. Brown spheres: Br. Blue spheres: Si.

terface is the hollow - top - hollow one, i.e., starting and ending at a hollow site, with the transition state being at a top site. The $BVSE$ was 0.13 eV. The pathways and the $BVSE$ are shown in Fig. 3 where we can see that the BVS has calculated three equivalent pathways energy-wise.

For the case with a MgI_2 substrate, the application of the BVS method showed that the energetically most favourable pathway for the Li-ion to migrate in the interface is the top - hollow - top one, i.e., starting and ending at a top site, with the transition state being at a hollow site. The $BVSE$ was 0.12 eV. The pathways and the $BVSE$ are shown in Fig. 4 where we can see that the BVS has calculated two equivalent pathways energy-wise.

IV. DISCUSSION

Applying the BVS method we found that the most conductive pathway for a Li ion in the interface between silicene and $MgCl_2$ and $MgBr_2$ substrates is the hollow - top - hollow one. This result is in agreement with the one derived by Zhu et al.[34] who applied DFT to calculate conductive pathways in the aforementioned materials and state that they found a local energy minimum at the top site. In addition, in the case of MgI_2 substrate, BVS showed that the top - hollow - top pathway is the most

favourable one, also in agreement with Zhu et al.[34].

Regarding the energy barriers for diffusion, BVS calculated a $BVSE$ of 0.15 eV, 0.13 eV and 0.12 eV for the cases with $MgCl_2$, $MgBr_2$ and MgI_2 substrates respectively. However, Li diffusion barriers using DFT were calculated[34] at 0.29 eV, 0.16 eV, 0.16 eV respectively. Therefore, there is an underestimation in the diffusion barriers. However, it is important to note that BVS preserved the trend regarding which material has smaller diffusion barrier. Add to that the fact that energy difference errors can exist in DFT that can be of the order of 0.2 eV[36,37] and the assumption of BVS this underestimation is logical.

The results presented above were extracted using a 3.4Å interface. In order to see how the diffusion barriers depend on the height of the interface, we repeated the process discussed in Section II for a 5Å interface. In this case, BVS calculated the exact same $BVSE$ for all substrates as with a 3.4Å interface. This is expected, because $BVSE$ calculations do not take under consideration the existence of Si atoms since the BVS method only cares about the cation - anion bonding between Li and the Cl, Br, I of the substrates. We should note that Zhu et al.[34], applying geometry optimization with DFT, found an interface of more than 3.2Å .

Initially, we took the Li ion positions to be those suggested in previous DFT studies[34]. However, we also ex-
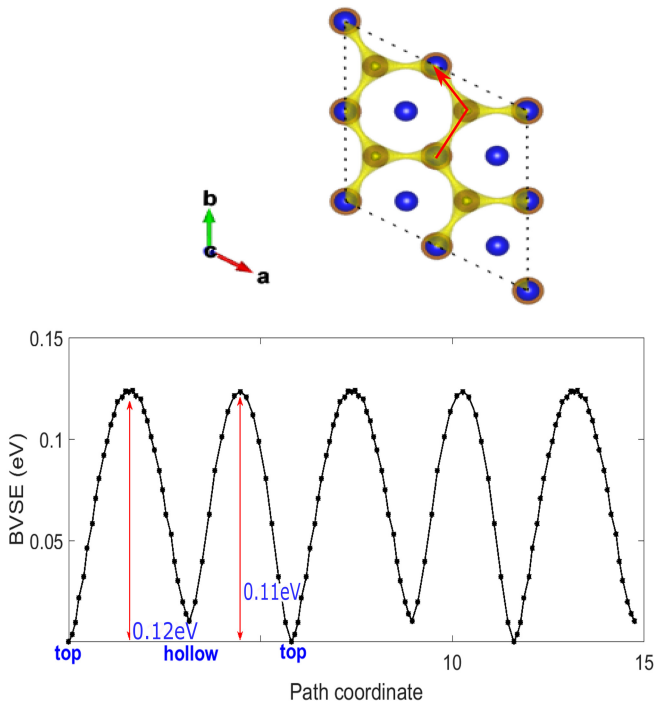
FIG. 4: Top panel: Top view of the $2 \times 2 \times 1$ supercell for the silicene with a MgI_2 substrate and the Li conductive pathways (yellow surface) as calculated by the BVS method. The arrow shows the direction of the migration. Bottom panel: The $BVSE$. Light brown spheres: Mg. Purple spheres: I. Blue spheres: Si.

amined different initial positions, namely the top positions for the $MgCl_2$ and $MgBr_2$ substrates and the hollow position for the MgI_2 substrate. BVS found the same results as the ones reported in Section III, adding validity to the fact that the method does not need the exact crystal structure.

Surface calculations: Apart from examining the Li ion diffusion in the interface, we also performed surface calculations. To that end, we placed the Li ion above the silicene layer. In this case the hollow position was now above the center of a Si hexagon while the top position was above a Si atom in the upper of the two silicene levels. For small interface distances, the results were the exact same as the ones in Section III. This was expected as, as we have already mentioned above, the BVS method does not take under consideration the Si atoms, therefore it does not care whether the silicene layer comes between Li and the substrates.

However, for interface heights larger than the bond length between Li-Cl, Li-Br and Li-I for each case of sub-

strates where there is no bonding between the Li ion and the substrates, the BVS method calculated no surface pathways. Therefore, BVS could be used to optimize the interface height, with calculations taking a small fraction of the computational cost of DFT or other computationally intensive methods.

V. CONCLUSIONS

In the present paper, we studied the diffusion pathways and energy barriers for a Li-ion in the interface between silicene and $MgCl_2$, $MgBr_2$ and MgI_2 substrates using the BVS method. We showed that BVS replicates the results previously published using DFT with great accuracy and time efficiency, while it is possible to avoid geometry optimization with DFT completely. In particular, BVS finished the calculations within a few minutes, whereas DFT took approximately two days, while the underestimation of the energy barrier of diffusion in the BVS model was insignificant when taking under consideration the $0.2\,\text{eV}$ error in DFT. In addition, surface calculations showed that the BVS method can also be used to roughly optimize the space between the silicene layer and the substrates. Therefore, we conclude that the BVS can be used to quickly find materials with low activation energies for ion diffusion, so that one can apply the time-consuming DFT calculations only to the materials needing detailed analysis.

A. Author Contributions

Konstantina A. Papadopoulou: Conceptualization, Methodology, Validation, Formal Analysis, Investigation, Resources, Data Curation, Writing-Original Draft, Visualization Alexander Chroneos: Conceptualization, Writing-Review & Editing, Project administration Stavros-Richard G. Christopoulos: Conceptualization, Methodology, Validation, Resources, Data Curation, Formal Analysis, Writing-Review & Editing, Supervision, Project administration, Funding acquisition

[*] Electronic address: S.R.Christopoulos@hud.ac.uk

[1] E. Scalise, M. Houssa, E. Cinquanta, C. Grazianetti, B. van den Broek, G. Pourtois, A. Stesmans, M. Fanci-

ulli, and A. Molle, 2D Materials **1**, 011010 (2014).

[2] L. Tao, E. Cinquanta, D. Chiappe, C. Grazianetti, M. Fanciulli, M. Dubey, A. Molle, and D. Akinwande, Nature

Nanotechnology **10**, 227 (2015).

3 J. Zhu, A. Chroneos, J. Eppinger, and U. Schwingenschlögl, Applied Materials Today **5**, 19 (2016).

4 J. Chapman, Y. Su, C. Howard, D. Kundys, A. Grigorenko, F. Guinea, A. Geim, I. Grigorieva, and R. Nair, Scientific Reports **6**, 1 (2016).

5 A. Molle, J. Goldberger, M. Houssa, Y. Xu, S.-C. Zhang, and D. Akinwande, Nature Materials **16**, 163 (2017).

6 E. Griffin, L. Mogg, G.-P. Hao, G. Kalon, C. Bacaksiz, G. Lopez-Polin, T. Zhou, V. Guarochico, J. Cai, C. Neumann, et al., ACS Nano **14**, 7280 (2020).

7 K. A. Papadopoulou, A. Chroneos, D. Parfitt, and S.-R. G. Christopoulos, Journal of Applied Physics **128**, 170902 (2020).

8 M. A. Kharadi, G. F. A. Malik, F. A. Khanday, K. A. Shah, S. Mittal, and B. K. Kaushik, ECS Journal of Solid State Science and Technology **9**, 115031 (2020).

9 C.-C. Liu, W. Feng, and Y. Yao, Physical Review Letters **107**, 076802 (2011).

10 C. Grazianetti, E. Cinquanta, and A. Molle, 2D Materials **3**, 012001 (2016).

11 F. Pan, Y. Wang, K. Jiang, Z. Ni, J. Ma, J. Zheng, R. Quhe, J. Shi, J. Yang, C. Chen, et al., Scientific reports **5**, 1 (2015).

12 Y. Cai, C.-P. Chuu, C. Wei, and M. Chou, Physical Review B **88**, 245408 (2013).

13 S. Chowdhury, A. Bandyopadhyay, N. Dhar, and D. Jana, Physical Sciences Reviews **2**, 20165102 (2017).

14 W. Kohn, A. D. Becke, and R. G. Parr, The Journal of Physical Chemistry **100**, 12974 (1996).

15 W. Wan and H. Wang, Materials **8**, 6163 (2015).

16 D. Vanderbilt, Physical Review B **41**, 7892 (1990).

17 H. Liu, J. Gao, and J. Zhao, The Journal of Physical Chemistry C **117**, 10353 (2013).

18 H. Liu, J. Gao, and J. Zhao, in *Journal of Physics: Conference Series* (IOP Publishing, 2014), vol. 491, p. 012007.

19 Z. Hong-Xia, Q. Ru-Ge, W. Yang-Yang, S. Jun-Jie, and L. Jing, Chinese Physics B **24**, 087308 (2015).

20 E. Scalise, K. Iordanidou, V. V. Afanas'ev, A. Stesmans, and M. Houssa, Nano Research **11**, 1169 (2018).

21 Y. Fan, X. Liu, J. Wang, H. Ai, and M. Zhao, Physical Chemistry Chemical Physics **20**, 11369 (2018).

22 C. Grazianetti and A. Molle, Research **2019** (2019).

23 H. Chen, L. L. Wong, and S. Adams, Acta Crystallographica Section B: Structural Science, Crystal Engineering and Materials **75**, 18 (2019).

24 I. D. Brown, Bond Valences pp. 11–58 (2013).

25 B. He, S. Chi, A. Ye, P. Mi, L. Zhang, B. Pu, Z. Zou, Y. Ran, Q. Zhao, D. Wang, et al., Scientific Data **7**, 1 (2020).

26 M. Avdeev, M. Sale, S. Adams, and R. P. Rao, Solid State Ionics **225**, 43 (2012).

27 J. Gao, G. Chu, M. He, S. Zhang, R. Xiao, H. Li, and L. Chen, Science China Physics, Mechanics & Astronomy **57**, 1526 (2014).

28 R. Xiao, H. Li, and L. Chen, Scientific Reports **5**, 1 (2015).

29 L. Pauling, Journal of the American Chemical Society **51**, 1010 (1929).

30 I. D. Brown, Chemical Reviews **109**, 6858 (2009).

31 S. Adams, Bulletin of Materials Science **29**, 587 (2006).

32 L. L. Wong, K. C. Phuah, R. Dai, H. Chen, W. S. Chew, and S. Adams, Chemistry of Materials **33**, 625 (2021).

33 S. Adams, Bond Valences pp. 91–128 (2013).

34 J. Zhu, A. Chroneos, and U. Schwingenschlögl, Nanoscale **8**, 7272 (2016).

35 H. Chen and S. Adams, IUCrJ **4**, 614 (2017).

36 A. Kushima, D. Parfitt, A. Chroneos, B. Yildiz, J. A. Kilner, and R. W. Grimes, Physical Chemistry Chemical Physics **13**, 2242 (2011).

37 B. Li, W. Gao, and Q. Jiang, Journal of Physics: Energy (2020).